Analysis of Electric Resistance of Diffusion-Welded Joint Based on Constriction Resistance†

Toshio ENJO*, Kenji IKEUCHI**, Naofumi AKIKAWA*** and Tsukasa OKAZAKI****

Abstract

New equations giving constriction resistance R_C as a function of area S_M and number density n of true contact spots have been obtained from a model experiment, and applied to the analysis of the electric resistance of the bond interface ΔR for the diffusion-welded joint of titanium. The new equations obtained are described as

$$R_C = \frac{\rho}{\sqrt{n}\cdot S}\left(\frac{\sqrt{\pi}}{2}\frac{\sqrt{S}}{\sqrt{S_M}} - 1.21\right) \quad \cdots\cdots (1)$$

for $(S_M/S) < 1/4$, and

$$R_C = \frac{\rho}{\sqrt{\pi n}\cdot S}\left\{\sqrt{\frac{S}{S_M}}\tan^{-1}\left(\sqrt{\frac{S}{S_M}} - 1\right) - 0.842\left(1 - \sqrt{\frac{S_M}{S}}\right)\right\} \quad \cdots\cdots (2)$$

for $(S_M/S) > 1/4$, where ρ is the resistivity of base metal and S the apparent contact area. It can be seen from these equations that parameter $A = (\Delta R\cdot S/\rho)$ depends only on (S_M/S) and n, if $\Delta R = R_C$. Parameter A measured at temperatures from 77K to room temperature for joints of titanium, however, decreased with a rise in the temperature of measurement, and its temperature dependence became less pronounced with the increase in welding temperature and time. On the other hand, area S_M and density n were estimated from fractured surfaces of joints on the assumption that spots where grooves caused by grinding of the faying surface were annihilated corresponded to true contact spots. Parameter A calculated from S_M and n thus obtained was significantly smaller than that measured at 77K and rather in good agreement with that measured at room temperature. This result indicates that not all the true contact spots observed on fractured surfaces corresponded to completely bonded spots having electrical properties identical with those of the base metal. The dependence of A on the temperature of measurement can be accounted for by a model that the bond interface consists of three characteristic spots: unbonded spot, completely bonded spot and incompletely bonded spot containing inclusions such as oxide films.

KEY WORDS: (Diffusion Welding) (Electric Resistance) (Constriction Resistance) (Titanium) (Bond Strength)

1. Introduction

The diffusion welding is a method by which materials can be bonded without melting or heavy plastic deformation in the bond zone. In such bond process, the microstructure of the bond interface and the resulting bond strength are considered to be strongly influenced by microscopic characteristics of the faying surface such as roughness and superficial oxide film[1]. The authors investigated the effects of the roughness and oxide film on the formation of true contact spots in the early process of diffusion welding by means of the electric resistance measurement across the bond interface[2,3]. In the investigation, the electric resistance across the bond interface was analyzed using the equation of constriction resistance given by[4]

$$R_C = \rho/(2\cdot a), \quad \cdots\cdots (1)$$

where R_C is the constriction resistance, ρ the resistivity of base metal, and a the radius of true contact spot. However, eq. (1) is a solution for contact resistance of a interface at which a couple of simi-infinite conductive members are in contact with each other in a circular spot[4], and so is valid only in the case where area of true contact spot S_M is much smaller than apparent contact area S.

An attempt to obtain an equation which was valid over a wider range than eq. (1) was made by R. Holm[5]. An approximate equation obtained by R. Holm, however, is not valid for $(S_M/S) > 0.3$, since Holm's equation gives negative constriction resistance in this range.

† Received on 2 May 1987.

* Professor
** Research Instructor
*** Graduate Student of Osaka University (Presently at Kawasaki Heavy Industries, Ltd.)
**** Graduate Student of Osaka University (Presently at Nippon Oil & Fats Co., Ltd.)

Transactions of JWRI is published by Welding Research Institute of Osaka University, Ibaraki, Osaka 567, Japan

The purpose of the present investigation is to expand the application of the constriction resistance to the analysis of the microstructure of bond interface. For this, an experimental equation of the constriction resistance which holds up to $(S_M/S) \sim 1$ has been obtained by a model experiment, and applied to the relation between the electric resistance of bond interface and the area and number of true contact spots for diffusion-welded joints of a commercially pure titanium.

2. Model Experiment on Constriction Resistance

The constriction resistance is generated at a place where the cross sectional area of a conductor is locally decreased, because current flow lines are bent together through the narrower area[4]. In other words, the resistance of a conductor having a locally narrower part consists of the constriction resistance in addition to the resistance given by the product of the resistivity by the size factor of the conductor (length/cross-sectional area). In the present investigation, the constriction resistance is estimated from a model experiment as described in the following section §2.1.

2.1 Measurement of constriction resistance

The specimen for the model experiment was a cold drawn bar of commercially pure aluminum 20mm in diameter and 300mm in length. As shown in **Fig. 1**, a circular notch of width $h \sim 1$ mm was cut in the specimen. The constriction resistance was estimated from the resistance between terminals 1 and 2 on both sides of the notch, and the resistivity of the specimen from the resistance between terminals 2 and 3. Terminals 4 and 5 were for passing the current through the specimen. The electric resistance measurement was carried out in stirred benzine at room temperature by the conventional potentiometric method as described in §3.1. The constriction resistance is estimated using the following equation:

$$R_C = R_{12} - \rho \cdot \left(\frac{2 \cdot l - h}{S_0} + \frac{h}{S_C}\right), \quad \cdots\cdots (2)$$

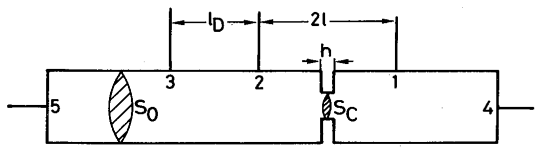

Fig. 1 Schematic diagram illustrating a notched specimen for the measurement of the constriction resistance. The cross-sectional area at the notch bottom S_C is assumed to correspond to the area of true contact spots S_M. Terminals 1, 2 and 3 are for the measurement of potential difference, and terminals 4 and 5 for the current supply.

where R_{12} is the resistance between terminals 1 and 2, $2l$ the distance between the terminals, S_0 the cross-sectional area of the specimen and S_C the cross-sectional area at the notch bottom. The resistivity ρ is given by

$$\rho = (S_0/l_D) \cdot R_{23}, \quad \cdots\cdots (3)$$

where R_{23} is the resistance between terminals 2 and 3 and l_D the distance between the terminals. The values of l, S_0, S_C and l_D were determined to an accuracy of $\pm 5\,\mu$m with a profile projector.

2.2 Estimation of constriction resistance from model experiment

The relation between constriction resistance and true contact area obtained from the model experiment is shown in **Fig. 2**. Dimensionless parameter $(R_C\sqrt{S_0}/\rho)$ is taken as the vertical axis in order to compensate the effects of resistivity ρ and cross sectional area S_0 on the constriction resistance. As shown in Fig. 2, the constriction resistance was increased with the increase in $\sqrt{S_0/S_C}$, i.e., the decrease in the ratio of true contact area to apparent contact area. For $\sqrt{S_0/S_C} > 2$, the relation between $R_C\sqrt{S_0}/\rho$ and $\sqrt{S_0/S_C}$ can be approximated by a straight line. For comparison, the relation of Eq. (1) and Holm's equation described as below[5]

$$R_C = \frac{\rho}{\sqrt{\pi S_0}}\left(\sqrt{\frac{S_0}{S_C}}\tan^{-1}\sqrt{\frac{S_0}{S_C}} - 2\right) \quad \cdots\cdots (4)$$

are also shown in Fig. 2.

As seen in Fig. 2, the constriction resistance is overestimated by the use of eq.(1) and underestimated by the use of Holm's equation. However, it should be noted that Holm's equation gives a relation nearly parallel to that obtained from the model experiment. Therefore, it will be possible to obtain an approximate equation for the con-

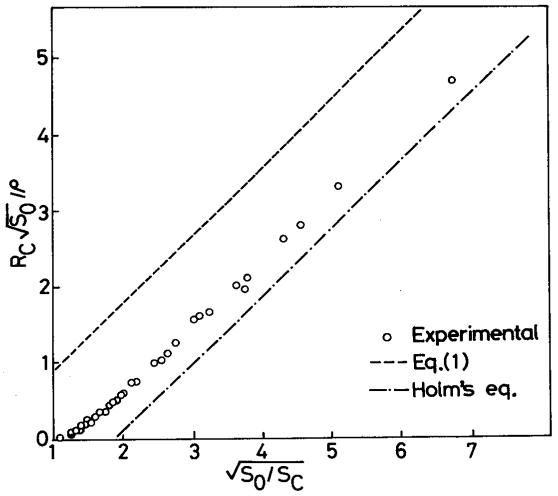

Fig. 2 Dimensionless parameter $(R_C\sqrt{S_0/\rho})$ vs $\sqrt{S_0/S_C}$, where R_C is the constriction resistance, and ρ the resistivity of the specimen.

striction resistance from Holm's equation by an appropriate modification. For $\sqrt{S_0/S_C} > 2$, since both the experimental relation and the relation given by Holm's equation can be well approximated by straight lines parallel to each other, the following equation can be derived:

$$R_C = \frac{\rho}{\sqrt{S_0}} \left(\frac{\sqrt{\pi}}{2} \sqrt{\frac{S_0}{S_C}} - 1.21 \right) . \quad \cdots\cdots\cdots\cdots \quad (5)$$

On the other hand, for $\sqrt{S_0/S_C} \leqslant 2$, Holm's equation is modified to the following equation:

$$R_C = \frac{\rho}{\sqrt{\pi S_0}} \left\{ \sqrt{\frac{S_0}{S_C}} \tan^{-1} \left(\sqrt{\frac{S_0}{S_C}} - 1 \right) - 0.842 \cdot \left(1 - \sqrt{\frac{S_C}{S_0}} \right) \right\} . \quad \cdots\cdots\cdots\cdots \quad (6)$$

As shown in **Fig. 3**, the constriction resistance given by eqs. (5) and (6) shows excellent agreement with the experimental.

Though the specimen for the model experiment corresponds to a joint having one true contact spot, a number of true contact spots are formed at the bond interface in actual diffusion welding (see Fig.8). According to Holm[5], the resistance of a bond interface having multiple true contact spots is given as the resistance of a circuit in which resistors corresponding to each true contact spots are connected in parallel. Suppose that N true contact spots of area (S_M/N) are distributed uniformly in a bond interface of apparent contact area S. Then, the constriction resistance of each true contact spot can be approximated by that of a bond interface which has a true contact spot of area (S_M/N) in apparent contact area (S/N). Consequently, from eqs. (5) and (6), the constriction resistance of a bond interface having true contact spots of number density $n = (N/S)$ is given by

$$R_C = \frac{\rho}{\sqrt{n \cdot S}} \left(\frac{\sqrt{\pi}}{2} \sqrt{\frac{S}{S_M}} - 1.21 \right) \quad \cdots\cdots\cdots\cdots \quad (7)$$

for $S_M/S \leqslant 1/4$, and

$$R_C = \frac{\rho}{\sqrt{\pi n S}} \left\{ \sqrt{\frac{S}{S_M}} \tan^{-1} \left(\sqrt{\frac{S}{S_M}} - 1 \right) - 0.842 \left(1 - \sqrt{\frac{S_M}{S}} \right) \right\} \quad \cdots\cdots\cdots\cdots \quad (8)$$

for $S_M/S > 1/4$.

The validity of Holm's treatment for multiple true contact spots has been established by a model experiment using rectangular-sheet specimens with multiple notchs[6].

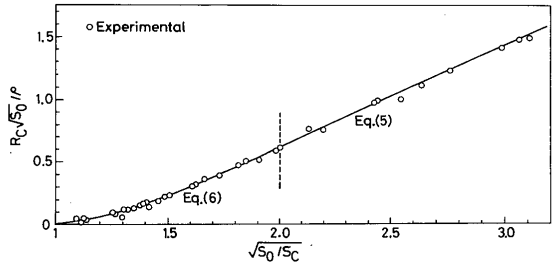

Fig. 3 Relation between $(R_C \sqrt{S_0}/\rho)$ and $\sqrt{S_0/S_C}$ given by eqs. (5) and (6).

3. Electric Resistance of Bond Interface in Diffusion-Welded Joint

3.1 Experimental details

The base metal used was a cold-drawn bar (20 mm in diameter) of commercially pure titanium with chemical composition as shown in **Table 1**. The specimen for the diffusion welding, a rod 20 mm in diameter and 37 mm in length, was cut from the base metal. The faying surface, the end surface of the rod, was finished by grinding on a metallographic paper of 800 grade, and washed in acetone just before the welding. Welding procedures employed were similar to those reported in a previous paper[7]; i.e., the bond interface was heated with a radiant resistance heater of molybdenum foil 0.1 mm thick, the welding pressure was applied to the bond interface with a hydraulic press, and the welding atmosphere was a vacuum of the order of 10^{-2}Pa.

The welded joint was cut to a cylindrical specimen 8 mm in diameter for the electric resistance measurement. As shown in **Fig. 4**, titanium wires (0.1 mm thick) 1, 2, 3 and 4 were percussion-welded to the specimen at a distance of about 10 mm as leads for the measurement of potential difference. The electric resistance measurement was carried out by a conventional potentiometric method as shown in Fig. 4: a direct current of 3–5 A was passed through the specimen, the potential difference between the leads was measured with a digital potentiometer to an accuracy of ±10 nV, and the electric resistance between the leads was estimated from the potential difference and current using Ohm's law. In the measurement, the direction of the current was reversed, and the mean value of the potential difference for each direction was employed for evaluating the resistance in order to compensate the

Table 1 Chemical composition of the base metal used (mass%).

Fe	N	O	H	Ti
0.038	0.0030	0.065	0.0028	Bal.

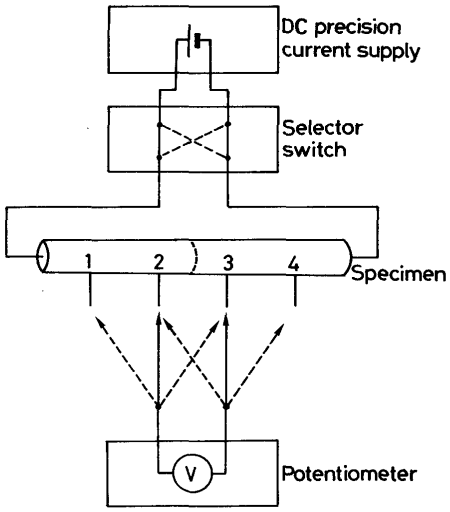

Fig. 4 Diagram illustrating the circuit for the electric resistance measurement of the bond interface. The electric resistance of the bond interface was estimated from the resistance between terminals 2 and 3, and the resistivity of the base metals from the resistance between 1 and 2 and the resistance between 3 and 4.

effect of the thermoelectric power on the measurement of the potential difference.

The electric resistance of the bond interface was estimated from electric resistance between leads 2 and 3 R_{23} by subtracting the resistance of the matrix metal:

$$\Delta R = R_{23} - \rho \cdot l_{23}/S, \quad \cdots\cdots (9)$$

where S is the cross sectional area of the specimen (~apparent contact area) and l_{23} the distance between leads 2 and 3. Resistivity ρ was determined from resistance between 1 and 2 R_{12} and between 3 and 4 R_{34} for each specimen. The measurement of the electric resistance was carried out in liquid baths kept at a desired temperature. The baths used were liquid nitrogen at 77 K and benzine at temperatures from 173 K to room temperature.

In the present investigation, parameter A given by the following equation was employed for describing the experimental result:

$$A = \Delta R \cdot S/\rho\ . \quad \cdots\cdots (10)$$

The reason for this is that A depends only on (S_M/S) and n from eqs. (7) and (8), if the electric resistance of bond interface ΔR is only due to the constriction resistance (if $\Delta R = R_C$). Therefore, if $\Delta R = R_C$, A is independent of the temperature of measurement. In the present investigation, A was measured at temperatures from 77 K to room temperature, in order to determine if $\Delta R = R_C$.

3.2 Results

The variation of A with welding time at welding temperatures from 1023 K to 1123 K is shown in **Fig. 5**,

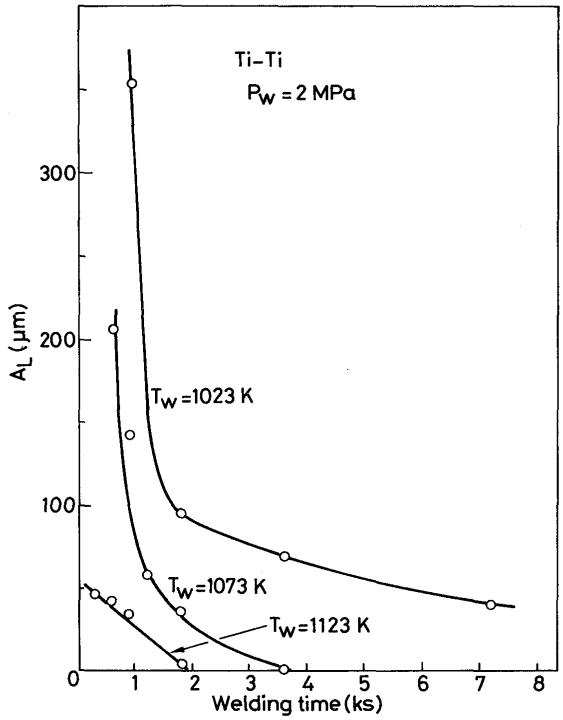

Fig. 5 Parameter A_L vs welding time at various welding temperatures T_W (A_L : A measured at 77 K, P_W : welding pressure).

where parameter A_L of the vertical axis indicates A measured at 77 K. As shown in Fig. 5, the value of A_L decreased with the increase in welding temperature and time, suggesting that the resistance of the bond interface decreased with the development of the bonding process.

In order to evaluate the contribution of the constriction resistance to the electric resistance of bond interface, the dependence of A on the temperature of measurement was investigated from 77K to room temperature. As shown in **Fig. 6**, parameter A decreased with the rise in the measurement temperature, suggesting that the contribution of factors other than the constriction resistance to the electric resistance of bond interface could not be neglected. In order to investigate the effect of welding parameters on the temperature dependence of A, difference between the values of parameter A measured at 77 K and at room temperature ΔA was plotted against welding time. As shown in **Fig. 7**, ΔA decreased as the welding temperature and time were increased. These results indicate that factors other than the constriction resistance have a considerable effect on the electric resistance of bond interface and that their contribution to the electric resistance of bond interface became less pronounced with the development of bonding process.

In order to examine the dependence of A on the temperature of measurement, experimental values of A were compared with values calculated by the use of eqs. (7) and (8). The ratio of true contact area to apparent contact area (S_M/S) and number density n to put into eqs.

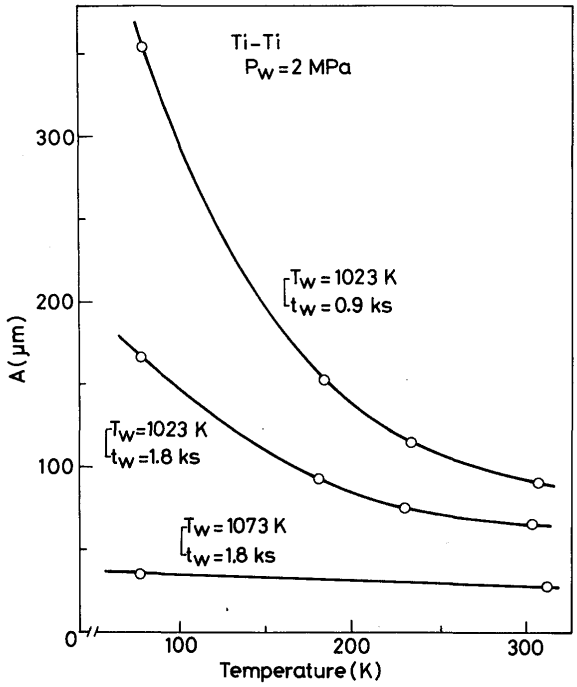

Fig. 6 Variation of A with the temperature of measurement (t_w : welding time).

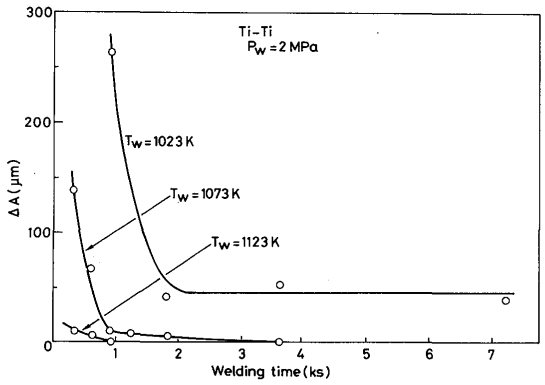

Fig. 7 Variation of $\Delta A = (A_L - A_R)$ with welding time, where A_R is parameter A measured at room temperature.

(7) and (8) were estimated from the observation of fractured surfaces of joints. The fractured surface, as shown in **Fig. 8**, consisted of two characteristic parts: dark parts where grooves caused by grinding of the faying surface still remained and bright parts where the groove was annihilated. The bright part can be regarded as a place where the bond is more or less fomed across the bond interface, since this part presents a dimple-like pattern. The ratio of true contact area (S_M/S) and number density n were estimated on the assumption that the bright part corresponded to the true contact spot.

In **Fig. 9**, products of A by $\sqrt{n}$ (A_L was measured at 77 K and A_R at room temperature) is plotted against $\sqrt{S/S_M}$ along with the theoretical relation (broken line) given by eqs. (7) and (8). As shown in Fig. 9, $A_R\sqrt{n}$ approximately obeyed the theoretical relation, though there

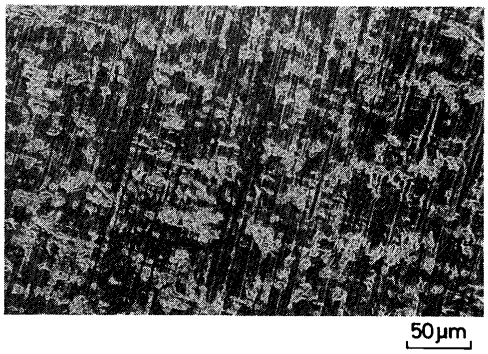

Fig. 8 Fractured surface of a joint after a tensile test (S_M/S = 30%, n = 6.9 × $10^8 m^{-2}$, T_w = 1023 K, t_w = 7.2 ks, P_w = 2 MPa).

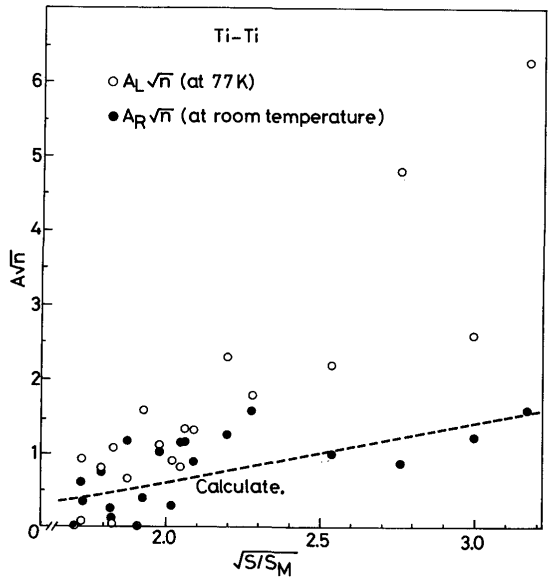

Fig. 9 $A\sqrt{n}$ ($A_R\sqrt{n}$: ●, $A_L\sqrt{n}$: ○) vs $\sqrt{S/S_M}$, where S_M and n were estimated from fractured surfaces as shown in Fig. 8. The broken line shows the relation given by eqs. (7) and (8).

is considerable scatter. On the other hand, $A_L\sqrt{n}$ took values much higher than the theoretical except for true contact ratio higher than 0.25 ($\sqrt{S/S_M} \leqslant 2$). This means that the electric resistance of bond interface at 77 K is much higher than that caused only by the constriction resistance when the true contact area is small. In other words, not all the true contact spot observed on the fractured surface corresponded to completely bonded spot having electrical properties identical with those of the base metal. This result was supported by the observation of the microstructure of bond interface and by the relation between the bond strength and true contact area as described below.

A microstructure of a bond interface in a joint for which (S_M/S) was estimated to be 30% from the fractured surface is shown in **Fig. 10**. If the place which was regarded as a true contact spot on the fractured surface was a completely bonded spot having identical properties with

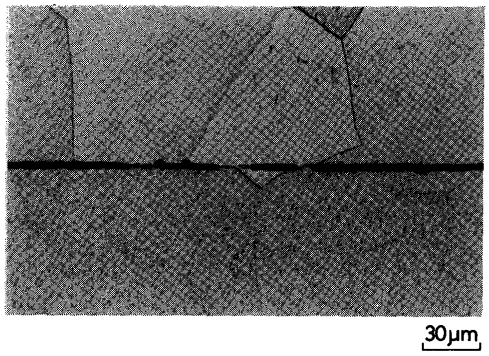

Fig. 10 Microstructure of a joint for which (S_M/S) was estimated to be 30% from the fractured surface (T_W = 1123 K, P_W = 2 MPa, t_W = 1.8 ks).

the base metal, the place would show features similar to those of the grain boundary in the base metal. As shown in Fig. 10, however, most of the bond interface appeared as a dark band thicker than the grain boundary, and the part showing features similar to the grain boundary was only about 10% of the bond interface. Therefore, the place which was regarded as the true contact spot by the observation of fractured surface included the spot with metallographic properties different from the base metal.

Figure 11 shows a relation between the bond strength and (S_M/S) obtained from the observation of fractured surface. As shown in the figure, a linear relation independent of welding parameters and the number of true contact spots was observed between the bond strength and (S_M/S). In Fig. 11, tensile strength of the base metal with a circular notch (see **Fig. 12**) is also shown for comparison with the bond strength. The ratio of true contact area (S_M/S) for the notched base metal is given by

$$(S_M/S) = (d/D)^2 \quad \cdots\cdots (11)$$

where D is the diameter of the specimen and d the diameter at the notch bottom. In order to apply a thermal history similar to that of the joint, the specimen of the base metal was held at 1073 K for 1.8 ks in a vacuum before being notched.

As shown in Fig. 11, the tensile strength of the joint and the notched base metal was almost the same at (S_M/S) of about 30%. However, the tensile strength of the joint decreased rapidly with the decrease in (S_M/S), and became much smaller than that of the notched base metal at (S_M/S) of about 10%. The sharpness and shape of the circular notch shown in Fig. 12 are, of course, quite different from those of the unbonded part in the bond interface. However, the fact that the tensile strength of the joint nearly equal to that of the base metal at (S_M/S) ~ 30% became much smaller at (S_M/S) ~ 10% suggested that the mean strength of the true contact spot observed on the fractured surface was considerably lower than that of the base metal at least for (S_M/S) ~ 10%. Therefore, it

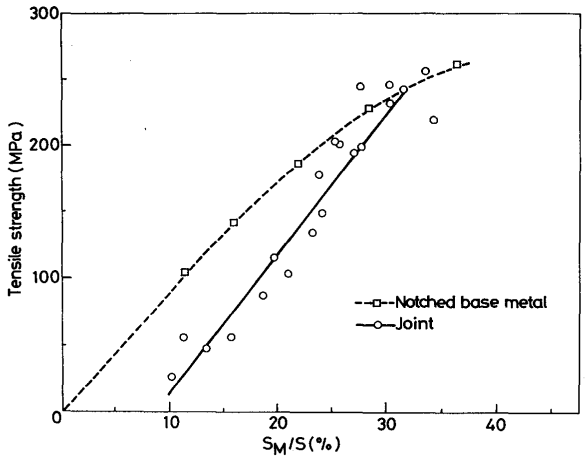

Fig. 11 Comparison between the bond strength of titanium and the strength of notched titanium bars. The ratio of cross-sectional area at the notch bottom to that of the bar $(d/D)^2$ is taken as (S_M/S) for the notched titanium bar (d and D: see Fig. 12).

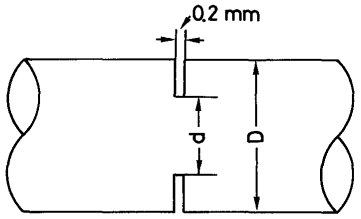

Fig. 12 Schematic diagram illustrating a notched titanium bar (D = 10 mm).

can be concluded that at (S_M/S) of about 10% the true contact spots observed on the fractured surface consist not only of completely bonded spots but also of incompletely bonded spots including microscopic defects such as oxide films and microvoids.

As shown in Fig. 9, the ratio of true contact area including these incompletely bonded spots could be estimated from A measured at room temperature. On the other hand, it still remains unknown what is estimated from A measured at 77 K. In **Fig. 13**, the bond strength is plotted against $A_L\sqrt{n}$ along with the tensile strength of the notched base metal. Parameter $A\sqrt{n}$ for the notched base metal is given by the substitution of $(d/D)^2$ for (S_M/S) in eqs. (7) and (8). As shown in Fig. 13, $A_L\sqrt{n}$ approximately obeyed the relation between $A\sqrt{n}$ and the strength for the notched base metal, though there is considerable scatter. This result implys that the contact area having the strength almost identical with that of the base metal is estimated from A measured at 77 K. As shown in Fig. 13, $A_R\sqrt{n}$ deviated significantly from the relation for the notched specimen at lower bond strength.

4. Discussion

From the results described in §3.2, it can be concluded that the contact spot at the bond interface of titanium

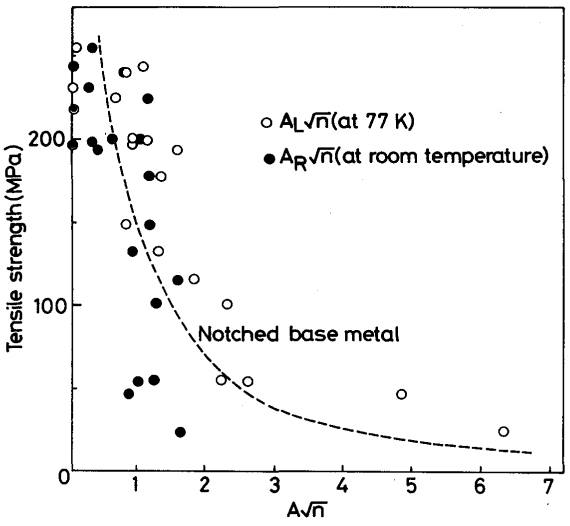

Fig. 13 Bond strength of titanium vs $A\sqrt{n}$ ($A_R\sqrt{n}$: •, $A_L\sqrt{n}$: o). The broken line shows the relation between the tensile strength of the notched titanium bar and $A\sqrt{n}$ estimated by substituting $(d/D)^2$ for (S_M/S) in eqs. (7) and (8).

can be classified into three types as schematically shown in **Fig. 14**: (a) completely bonded spot having properties identical with those of the base metal, (b) intermediate state between (a) and (c), and (c) incompletely bonded spot including defects such as oxide films and microvoids. As a typical example, the temperature dependence of A is calculated below for a bond interface having three contact spots each of which corresponds to those shown in Fig. 14 (a), (b) and (c).

In this case, three resistors corresponding to each contact spot can be considered to be connected in parallel across the bond interface, and so the electric resistance across the bond interface ΔR is approximately given by

$$\frac{1}{\Delta R} = \frac{1}{\Delta R_1} + \frac{1}{\Delta R_2} + \frac{1}{\Delta R_3}, \quad \cdots\cdots (12)$$

where ΔR_1, ΔR_2 and ΔR_3 are the electric resistance of the contact spots shown in Fig. 14 (a), (b) and (c), respectively. From eqs. (10) and (12), A satisfys the following equation:

$$\frac{1}{A} = \frac{1}{S}\left(\frac{\rho}{\Delta R_1} + \frac{\rho}{\Delta R_2} + \frac{\rho}{\Delta R_3}\right). \quad \cdots\cdots (13)$$

In this equation, since ΔR_1 is due to the constriction resistance, $(\rho/\Delta R_1)$ is independent of the temperature of measurement and does not cause the temperature dependence of A. On the other hand, the electric resistance of the incompletely bonded spot ΔR_3, which consists of the resistance due to microscopic defects r_b as well as the constriction resistance r_c, is approximated by the following equation:

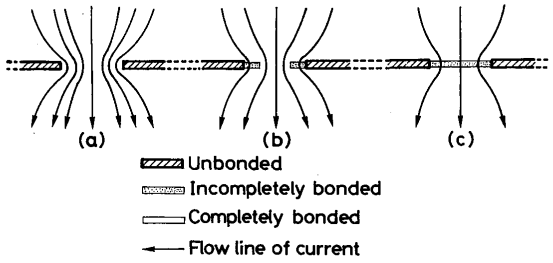

Fig. 14 Schematic diagram illustrating the model of the bond interface of titanium.

$$\Delta R_3 = r_c + r_b. \quad \cdots\cdots (14)$$

Therefore,

$$\rho/\Delta R_3 = 1/(r_c/\rho + r_b/\rho). \quad \cdots\cdots (15)$$

In eq. (15), since constriction resistance r_c is proportional to ρ, the temperature dependence of A is controlled by (r_b/ρ).

If electric resistance r_b is due to the titanium oxide TiO_2 originating from the superficial oxide film, r_b will decrease with the rise in temperature similarly to that of TiO_2[8]. The electric resistance of $TiO_{1.01\sim0.85}$[9] has been reported to increase with temperature, but its increasing rate $\Delta\rho/\rho$ ($\Delta\rho$: increase in ρ due to increase in temperature ΔT) is much smaller than that of titanium. Therefore, if the resistance r_b is due to the titanium oxide TiO_2 or $TiO_{1.01\sim0.85}$, (r_b/ρ) will decrease with the rise in temperature. Since A decreases with (r_b/ρ) from eqs. (13) and (15), the temperature dependence of A as shown in Fig. 6 can be explained qualitatively as a consequence of r_b caused by the titanium oxide.

The increase in (r_b/ρ) results in the decrease in the contribution of the incompletely bonded spot $(\rho/\Delta R_3)$ to A value from eqs. (13) and (15). In other words, the contribution of the incompletely bonded spot to A value decreases with the decrease in temperature, if r_b is due to the titanium oxide. It is probably for this reason that the contact area having strength almost identical with that of the base metal is estimated from A measured at 77 K as shown in Fig. 13.

A contact spot at which completely and incompletely bonded parts coexist is shown in Fig. 14 (b). In this case, when the electric resistance measurement is carried out at very low temperature, the electric resistance of the incompletely bonded part becomes much higher than that of the completely bonded part, and almost all current flow lines pass through the completely bonded part. On the other hand, at very high temperatures, the difference in the electric resistance between the completely and incompletely bonded parts becomes small, and flow lines pass through the incompletely bonded part as well as the

completely bonded. That is, for the contact spot as shown in Fig. 14 (b), the rise in temperature has virtually an effect similar to the increase in the true contact area S_M and results in the decrease in A from eqs. (7) and (8).

Thus, the dependence of A on the temperature of measurement can be qualitatively accounted for by the model of the bond interface as shown in Fig. 14.

5. Conclusions

In the present investigation, experimental equations which give the constriction resistance as a function of area and number of true contact spots have been obtained from a model experiment. The equations obtained have been applied to the diffusion-welded joint of a commercially pure titanium in order to examine the microstructure of the bond interface by the electric resistance measurement across the bond interface. Results obtained are summarized as follows:

(1) The equations obtained are described as follows:

$$R_C = \frac{\rho}{\sqrt{n}\,S}\left(\frac{\sqrt{\pi}}{2}\sqrt{\frac{S}{S_M}} - 1.21\right) \cdots\cdots\cdots (16)$$

for $(S_M/S) \leqslant 1/4$, and

$$R_C = \frac{\rho}{\sqrt{\pi n}\,S}\left\{\sqrt{\frac{S}{S_M}}\,\tan^{-1}\left(\sqrt{\frac{S}{S_M}} - 1\right) - 0.842\left(1 - \sqrt{\frac{S_M}{S}}\right)\right\} \cdots\cdots\cdots\cdots (17)$$

for $(S_M/S) > 1/4$, where R_C is the constriction resistance, ρ the resistivity, S the apparent contact area, S_M the area of true contact spots and n the number density of true contact spots. If the electric resistance of bond interface ΔR is caused only by the constriction resistance ($\Delta R = R_C$), parameter $A = (\Delta R \cdot S/\rho)$ depends only on (S_M/S) and n as seen from eqs. (16) and (17).

(2) Parameter A for the diffusion-welded joint of titanium decreased with the rise in the temperature of measurement, suggesting that the electric resistance of bond interface was influenced considerably by factors other than the constriction resistance. The temperature dependence of A became smaller with the increase in welding temperature and time.

(3) The temperature dependence of A can be explained by the model that true contact spots of three types are formed at the bond interface as shown in Figs. 14 (a), (b) and (c) : (a) completely bonded spot having properties identical with those of the base metal, (b) intermediate spot at which completely and incompletely bonded parts coexist and (c) incompletely bonded spot including defects such as microvoids and titanium oxides. Among these, (b) and (c) spots can cause the temperature dependence of A as described in (2), if their electric resistance is influenced significantly by the titanium oxide; for the electric resistance of the oxide generally decreases with the rise in temperature. The model of the bond interface shown in Fig. 14 has been supported by the comparison of experimental A values with those calculated from area and number of true contact spots observed on the fractured surface.

References

1) M. M. Schwartz: *Modern Metal Joining Techniques,* John Wiley & Sons, (1969), 370.
2) T. Enjo, K. Ikeuchi and N. Akikawa: Trans. JWRI, **10** (1981), 173.
3) T. Enjo, K. Ikeuchi and N. Akikawa: Trans. JWRI, **11** (1982), 49.
4) R. Holm: *Electric Contact Handbook,* Springer-Verlag, (1958), 17.
5) R. Holm: *Electric Contact Handbook,* Springer-Verlag, (1958), 22.
6) N. Akikawa: Dr. Thesis, Faculty of Engineering, Osaka University, (1983) (in Japanese).
7) T. Enjo, K. Ikeuchi and T. Horinouchi: Trans. JWRI, **15** (1986), 61.
8) Z. M. Jarzębski: *Oxide Semiconductors,* Pergamon Press, (1973), 212.
9) S. Takeuchi and K. Suzuki: J. Japan Inst. Metals, **33** (1969), 284 (in Japanese).